JOURNAL OF COMPUTATIONAL PHYSICS 50, 447–481 (1983)

Upwind Schemes and Boundary Conditions with Applications to Euler Equations in General Geometries

STANLEY OSHER*

Department of Mathematics,
University of California, Los Angeles, Los Angeles, California 90024

AND

SUKUMAR CHAKRAVARTHY

Department of Aeronautics/Astronautics, Stanford University, Stanford, California 94305

Received April 20, 1982; revised October 13, 1982

A unified treatment of several upwind shock capturing algorithms is presented. Each algorithm has a Riemann initial value problem as its basis. The treatment of boundaries involves solving the associated Riemann initial-boundary value problem. The first author's algorithm, applied to multidimensional Euler equations in general geometries, is then presented. Its worth is verified by various calculations, which include Mach 8 supersonic flow past a circular cylinder.

1. INTRODUCTION

Coventional implicit finite difference methods based on central difference approximations of the spatial derivative terms in the Euler equations are prone to failure when "capturing" strong shocks. They also need an artificial dissipation term, the coefficient of which must be judiciously chosen for convergence. Conventional explicit schemes based on the Lax–Wendroff discretization also suffer from a similar lack of robustness in computing complex flows with shock waves and steep gradients. While these schemes have been widely used on a variety of problems (see [3] for references) that list of solved problems does not include flows with strong shocks (say Mach 5 upstream, normal to the shock), when the shocks are captured.

A main drawback of most finite-difference schemes is that discontinuities are approximated by discrete transitions, that when narrow, usually overshoot or undershoot, or when monotone, usually spread the discontinuity over many grid points.

* Research partially supported by NSF Research Grant MCS 78-0152.

0021-9991/83 $3.00

Upwind difference algorithms have been designed and used over the years, largely because of their success in treating this difficulty. In particular the Murman–Cole scheme [14] has been the main element of successful production codes, used to solve the small disturbance equation of transonic flow throughout the world.

Although this scheme does treat discrete shocks very well, it has a different drawback—it possesses numerically stable, nonphysical expansion shocks.

Engquist and Osher [5–7], developed, circa 1980, a monotone upwind scheme for scalar conservation laws and applied it to the small disturbance equation of transonic flow. Osher then developed a generalization of the scalar algorithm for hyperbolic systems of conservation laws [16], which was further studied by Osher and Solomon [19].

The Osher scheme for systems is an upwind shock "capturing" algorithm applied to the unsteady Euler equations. It resembles several others, such as Godunov's [8], Roe's [21], and Steger and Warming's [20]. It can be applied to essentially all hyperbolic systems of conservation laws arising in physics, but becomes relatively simple for Euler's equations in general geometries using body fitted coordinates. The precise algorithm will be given in Sections II and IV.

The Osher scheme is based on a Riemann solver, as is Godunov's, but compression and rarefaction waves are used to approximate shocks. This leads to a simpler and smoother algorithm. The numerical flux functions, which are at least continuously differentiable, are written in closed form, and include various switches which make them upwind. The algorithm reaches steady shock solutions exactly (for constant states in either side of the shock) on the grid with a one or two point monotone transition. The existence and a uniqueness result for these discrete shocks was given in [19], as was a proof that limit solutions satisfy the entropy condition.

Geometric properties of discrete shocks for Godunov's, Roe's, and Osher's schemes were analyzed in [17]. The sharp monotone profiles property holds in several space dimensions in general geometries for Osher's scheme if each one dimensional operator "sees" a shock. This was shown numerically in [19] for the isentropic Euler equations in cartesian coordinates, in [17], both analytically, and numerically for scalar problems, and in this work and in [3] for the full Euler equations in various geometries. The last calculations are presented in Section VI.

Reference [3] is a parallel work to this one, in which we present the algorithm, the results of various calculations, and emphasize the aerodynamical aspects of this method.

The outline of this paper is as follows: In Section II, we review upwind schemes, stressing Godunov's method which uses the Riemann initial value problem. We then review Osher's scheme for general systems in one space dimension of the form

$$q_t + f(q)_x = 0. \tag{1.1}$$

In Section III we present and analyze a method for treating computational and physical boundaries based on solving the initial-boundary value Riemann problem. This applies directly (in different ways) to interior differencing using either

Godunov's or Osher's methods. In Section IV we present the closed form Osher algorithm for Euler's equations in general geometries (including moving coordinate systems), for both the interior and boundary differencing. Three basic forms of the differencing, which are very similar, are presented. It is proven in the Appendix that all limit solutions satisfy the correct jump conditions. This is not completely obvious, because of the involvement of the independent variables as a result of coordinate changes. The relative merits of the three approaches are discussed. Boundary conditions for Euler's equations in general geometries are given in Section V.

In Section VI we discuss the results of various calculations. These are also presented in Figs 3 to 12. Besides the strong shock results for one space dimension, we mention here the particular case of two-dimensional Mach 8 flow past a circular cylinder. The crispness of the shock transition is obvious (Figs. 8 and 9) and the agreement with a shock "fitted" solution obtained by Lyubimov and Rusanov [18] is quite good (Figs. 9 and 10). Other accurate calculations are presented in this section, including duct flow through a Laval nozzle and supersonic flow past a wedge airfoil. More examples are given in [3].

Section VII contains some comparisons and conclusions.

In future work we shall present implicit implementations of this algorithm, and a treatment of second order accuracy.

II. Review of Upwind Schemes

We begin with Godunov's approximation to

$$q_t + f(q)_x = 0, \qquad t > 0, \ -\infty < x < \infty, \tag{2.1}$$

with initial data $q(x, 0)$ given.

Here

$$q = (q_1, \ldots, q_d)^T, \qquad f(q) = (f_1(q), \ldots, f_d(q))^T,$$

and the Jacobian matrix $\partial f(q) = A(q)$ has real eigenvalues

$$\lambda_1(q) \leqslant \lambda_2(q) \leqslant \cdots \leqslant \lambda_d(q),$$

where each λ_i is repeated according to its multiplicity.

We set up the rectangular lattice made up of

$$\begin{aligned} \Omega_{jn} &= \{(x, t) \mid x_{j-1/2} \leqslant x < x_{j+1/2}, \ t^n \leqslant t < t^{n+1}\} \\ &= \mathscr{I}_j \times \mathscr{T}^n, \end{aligned}$$

where, for simplicity, we take $x_j = j\,\Delta x$, $t^n = n\,\Delta t$ with j, n any integers, $n \geqslant 0$.

We wish to construct an approximate solution which is piecewise constant, with

$$q_j^n \sim q(x, t) \qquad \text{in} \quad \Omega_{j,n}.$$

Godunov in [8] does this as follows. Given $q(x, 0)$ for x in $\mathscr{I}_j$, let

$$q_j^0 = \frac{1}{\Delta x} \int_{\mathscr{I}_j} q(x, 0)\, dx$$

be the approximate solution in $\Omega_{j,0}$. Then we advance the approximate solution in time by solving a sequence of Riemann problems.

A Riemann problem for (2.1) is defined to be an initial value problem, with piecewise constant initial data of the type

$$q(x, 0) \equiv q^{\mathrm{L}} \qquad \text{for} \quad x < 0$$
$$q(x, 0) \equiv q^{\mathrm{R}} \qquad \text{for} \quad x \geqslant 0.$$

Lax, in [11], has constructed the solution to (2.1) for $|q^{\mathrm{L}} - q^{\mathrm{R}}|$ small enough, given certain hypotheses concerning strict hyperbolicity, genuine nonlinearity, and linear degeneracy. For the moment, we only assume that a solution exists, which is physically correct, and which is of the form $q(x, t) = q(x/t)$, a similarity solution.

Then Godunov's algorithm continues by solving the initial value problem with piecewise constant data throughout. For $\lambda = \Delta t/\Delta x$ sufficiently small (the CFL condition), there is no interaction between different Riemann problems, and a solution $q_\Delta(x, t)$ is obtained for all x, and $0 \leqslant t \leqslant \Delta t$.

Then q_j^1 is defined to be the space average of $q_\Delta(x, t)$ over $\mathscr{I}_j$ at $t = \Delta t$:

$$q_j^1 = \frac{1}{\Delta x} \int_{\mathscr{I}_j} q_\Delta(x, t^1)\, dx.$$

Repeating gives us

$$q_j^{n+1} = \frac{1}{\Delta x} \int_{\mathscr{I}_j} q_\Delta(x, t^{n+1})\, dx.$$

If (2.1) is integrated around $\Omega_{j,n}$, the expression above may be written in closed form as

$$q_j^{n+1} = q_j^n - \lambda(f_{j+1/2}^n - f_{j-1/2}^n), \tag{2.2}$$

where $f_{j+1/2}^n = f(q(x_{j+1/2}, t))$, for any t strictly between t^n and t^{n+1}. The function q_Δ is constant there, since we have a similarity solution. Scheme (2.2) is said to have the conservation form.

To appreciate approximate solutions to Riemann's problem, consider the linear case: $f(q) = Aq$, with A a constant matrix which we take to be diagonal,

$$A = \begin{pmatrix} A^0 & 0 & 0 \\ 0 & A^+ & 0 \\ 0 & 0 & A^- \end{pmatrix} \tag{2.3}$$

with Λ^0 a $d_0 \times d_0$ null matrix, Λ^+ a $d_+ \times d_+$ positive definite matrix, and Λ^- a $d_- \times d_-$ negative definite matrix.

Let P^0, P^+, P^- be the natural projections onto the corresponding invariant subspaces of A. Then, Godunov's method is easily seen to reduce to

$$q_j^{n+1} = q_j^n - \lambda[P^+ A(q_j^n - q_{j-1}^n) + P^- A(q_{j+1}^n - q_j^n)], \tag{2.4}$$

so $f_{j+1/2} = P^+ A q_j + P^- A q_{j+1}$, in this case.

This is the well known Courant–Isaacson–Rees upwind scheme [4] for the linear equation. For nonlinear problems, a scheme of this type is often used, i.e., the algorithm is of the form

$$q_j^{n+1} = q_j^n - \lambda(P_{j,n}^+ A(q_j^n)(q_j^n - q_{j-1}^n) + P_{j,n}^- A(q_j^n)(q_{j+1}^n - q_j^n)), \tag{2.5}$$

where the Jacobian matrix, $A(q)$, is linearly equivalent to a matrix of type (2.3) at each q_j^n, and the $P_{j,n}^+$, $P_{j,n}^-$ are the natural projections onto these subspaces; see, e.g., [2].

Unfortunately, this scheme is not in conservation form, i.e., it is not of type (2.2) above, for some numerical flux functions $f_{j-1/2}, f_{j+1/2}$. Thus, it must be used together with shock fitting at discontinuities. This has also been done in [2].

The proper nonlinear conservation form of (2.4) was given by van Leer [24], and follows after introducing the matrix $|A| = P^+ A - P^- A$. The scheme is of form (2.2), with (dropping superscripts)

$$f_{j+1/2} = \tfrac{1}{2}\{f(q_{j+1}) - f(q_j) - |A|_{j+1/2}(q_{j+1} - q_j)\}, \tag{2.5a}$$

where $|A|_{j+1/2}$ is some unspecified average, or representative value, of A on the interval (q_j, q_{j+1}).

A scheme in conservation form allows for "shock capturing." The Lax–Wendroff theorem [12], guarantees that limit solutions will be weak solutions of (2.1) and the correct jump conditions across discontinuities will be obtained. Moreover, for a wide class of physically interesting problems, including those studied below, limit solutions will be physically correct—expansion shocks are ruled out.

One difficulty with Godunov's scheme lies in its complexity. The Riemann problem is often difficult to obtain in closed form. In consequence, users of the scheme, including Godunov [23], have simplified it by using an approximate solution to the Riemann problem. In [23], the "shocks only" approximation was introduced: rarefaction waves in the Riemann solution are replaced by expansion shocks. This is a dangerous procedure, since the expansion shocks may show up.

A special averaging routine was recently suggested by Roe [21]. Given two vectors q^L, q^R, Roe defines a matrix $A(q^L, q^R)$, such that $\lim_{q^L \to q^R} A(q^L, q^R) = \partial f(q^R)$ and

$$f(q^L) - f(q^R) = A(q^L, q^R)(q^L - q^R). \tag{2.6}$$

For $d > 1$ there may be many such matrices. One candidate is always

$$A(q^L, q^R) = \int_0^1 A(q^R + s(q^L - q^R))\, ds,$$

for which (2.6) is easily verified. Harten [25] proved that this matrix has real eigenvalues, for a wide class of equations. Roe's choice is based on computational simplicity.

Roe's scheme of form (2.2) is then generated by

$$f_{j+1/2} = \tfrac{1}{2}[f(q_{j+1}) + f(q_j) - |A(q_j, q_{j+1})|\,(q_{j+1} - q_j)|. \tag{2.7}$$

This scheme is, in general, much simpler than Godunov's. It is also in conservation form. However, it allows limit solutions which possess expansion shocks, because of (2.6), and these are obtained in a stable fashion. In fact, for the scalar case, with $f(q) = \frac{1}{2}q^2$, this reduces to the Murman–Cole scheme using Murman's shock and sonic point operators [14], which is well known to possess these stable nonphysical solutions [10]. The Murman–Cole scheme is a "shocks only" Godunov method, for a special scalar convex conservation law.

One positive attribute of both Godunov's and Roe's approximations is the exact resolution, for for one transition point, of zero speed physically correct shock solutions, to their schemes.

Finally, we discuss Osher's [16] scheme, which is also of form (2.5a). It is an extension to systems of the scheme developed by Engquist and Osher [5–7], for a single conservation law, $d = 1$, in (2.1),

$$f_{j+1/2} = \tfrac{1}{2}\left[f(q_{j+1}) + f(q_j) - \int_{q_j}^{q_{j+1}} |f'(q)|\, dq\right]. \tag{2.8}$$

If we define

$$f_+(q) = \int_0^q \max(f'(s), 0)\, ds,$$

$$f_-(q) = \int_0^q \min(f'(s), 0)\, ds,$$

then scheme (2.2) with this numerical flux function is such that

$$f_{j+1/2} - f_{j-1/2} = \Delta_+ f_-(q_j) + \Delta_- f_+(q_j)$$

with $\Delta_\pm h_j = \pm(h_{j\pm 1} - h_j)$ defining the usual difference operators. This is, therefore, a flux splitting algorithm.

Van Leer, in [22], pointed out a geometric interpretation of the E.–O. scheme which makes it a Riemann solver—Godunov type algorithm. Namely, for convex $f(u)$, the Riemann problem is solved, not using rarefaction and shock waves, but

using rarefaction and compression waves. This is done by letting the compression waves overturn, and a multi-valued solution is generated. The averaging procedure is done over this multi-valued, but continuous, solution manifold. This leads precisely to flux function (2.8). The E.–O. scheme is, therefore, a "simple waves only" Godunov scheme. Like the full Godunov scheme, it rules out expansion shocks and, in fact, enforces an entropy inequality.

Osher extended (2.8) to strictly hyperbolic systems (distinct real eigenvalues of $\partial f(q)$) by replacing $f'(q)$ by $\partial f(q)$, and defining the path of integration, in phase space, as follows.

Let $\lambda_1 < \lambda_2 < \cdots < \lambda_d$ be the eigenvalues of ∂f, and let $r_1, r_2, \ldots, r_d$ be the corresponding right eigenvectors.

Consider a solution in d dimensional phase space of the system of ordinary differential equations

$$\frac{dq}{ds} = r_k(q(s)). \tag{2.9}$$

(Here s is just arc length.)

Along such a path Γ_k, the integrand in (2.8) simplifies to

$$|\partial f(q)|\, dq = |\lambda_k|\, r_k\, ds.$$

For Euler's equations and many other physical systems, the fields are either genuinely nonlinear, which means that r_k can be normalized so that $\nabla_q \lambda_k \cdot r_k \equiv 1$, or linearly degenerate, for which $\nabla_q \lambda_k \cdot r_k \equiv 0$.

For a linearly degenerate field, λ_k is constant on the orbit of (2.9) and

$$\int_{\Gamma_k} |\partial f(q)|\, dq = (\operatorname{sgn} \lambda_k) f(q) \Big]_{q^B}^{q^u}, \tag{2.10}$$

where q^u, q^B are the upper and lower limits of integration.

For a genuinely nonlinear field, λ_k is a monotone function of arc length on an orbit of (2.9). This means, among other things, that there exists exactly one point along Γ_k or its extension, for which λ_k vanishes. There is a unique $\bar{q}$ for which $\lambda_k(\bar{q}) = 0$ and $\bar{q}$ is connected to q^u and q^B through an orbit of (2.9).

It is then easy to show

$$\int_{\Gamma_k} |\partial f(q)|\, dq = 2f(q) \Big]_{\substack{q^u \text{ if } \lambda_k(q^u) > 0 \\ \bar{q} \text{ if } \lambda_k(q^u) \leq 0}}^{\substack{q^B \text{ if } \lambda_k(q^B) > 0 \\ \bar{q} \text{ if } \lambda_k(q^B) \leq 0}} - f(q) \Big]_{q^B}^{q^u}. \tag{2.11}$$

The path Γ^j connecting q_j to q_{j+1} in (2.8) is then taken to be a continuous piecewise smooth union of segments Γ_k^j. We begin with $k = d$ in (2.9) emanating from q_j. Then stop at some end state and use this end value as initial value for (2.9) with $k = d - 1$. Continue until, for $k = 1$, the last segment Γ_1^j ends at q_{j+1}. By the implicit function theorem, there exists a unique path if $|q_{j+1} - q_j|$ is sufficiently small.

Thus (2.8) is well defined, and just as in the scalar case, the numerical flux functions each consist of the average flux $(f(q_j)+f(q_{j+1}))/2$ modified by the addition of flux differences of $f(q)$, for certain q on this path, which correspond either to sign changes of $\lambda_k(q)$ (sonic points), or sign changes from one λ_k to the next λ_{k+1}.

The details have been worked out for certain physical examples, including one-dimensional, compressible, nonisentropic Eulerian gas flow in [19] and also two-dimensional, compressible, isentropic gas flow.

Desirable theoretical and computational properties (including no nonphysical limit solutions) were obtained there, and some were extended in [17]. In particular, monotone, sharp, steady profiles, with a two point, rather than one point, transition region, were found, and were shown to be essentially unique. Moreover, in general, $d-1$ independent functions of q were shown to have only a one point transition region for these discrete shocks. (For the example above, these are the entropy p/p^{γ}, and one of the functions $u \pm (2/(\gamma-1))c$.)

The k Riemann invariants act as building blocks for the scheme, since for each k, they are $d-1$ independent functions constant on Γ_k.

It is often desirable to use implicit methods to approximate (2.1). A standard procedure is to being with a method of lines semi-discrete approximation

$$\frac{\partial q_j}{\partial t} = -\frac{1}{\Delta x}(f_{j+1/2} - f_{j-1/2}) = -\frac{1}{\Delta x}\Delta_+ f_{j-1/2}, \tag{2.12}$$

where the numerical flux function is of the form

$$f_{j-1/2} = h(q_j, q_{j-1}).$$

One might, for example, use backwards Euler time integration:

$$\frac{q_j^{n+1} - q_j^n}{\Delta t} = -\frac{1}{\Delta x}\Delta_+ h(q_j^{n+1}, q_{j-1}^{n+1}). \tag{2.13}$$

Other possible time discretizations include Crank–Nicolson.

To solve the resulting nonlinear system of equations for $q^{n+1} = \{q_j^{n+1}\}_{j=-\infty}^{\infty}$, one usually linearizes and uses Newton's method, with the initial guess q^n, the value at the former time level. Such a method will converge quadratically near steady state, given some smoothness on the flux functions $h(q_j, q_{j-1})$. Unfortunately, for both Roe's and Godunov's schemes, the flux function fails to be differentiable whenever q_j and q_{j+1} are connected by a steady shock. This makes implicit methods problematic. The E.–O. scheme has (at least) continuous first partial derivatives, as does Osher's extension to systems. This may help explain its superior robustness for the implicit aerodynamic calculations performed in [9], and elsewhere. The differentiability also makes this scheme more easily accessible for numerical analysis than for Roe's or Godunov's methods.

For future use, we rewrite the flux difference resulting from the expression for systems in (2.8) as

$$f_{j+1/2} - f_{j-1/2} = \int_{q_{j-1}}^{q_j} (\partial f)^+ \, dq + \int_{q_j}^{q_{j+1}} (\partial f)^- \, dq, \tag{2.14}$$

where $(\partial f)^+ = P^+ \, \partial f$, $(\partial f)^- = P^- \, \partial f$, and the paths of integration are Γ^{j-1} and Γ^j, respectively.

III. Boundary Conditions for Upwind Schemes

We now turn to the implementation of both physical and computational boundary conditions for upwind schemes. The treatment below is an extension of Godunov's [8, 23] boundary treatment to general boundary conditions and general hyperbolic systems.

We consider problem (2.1) to be solved in a quarter space, $t > 0$, $x > 0$, with given initial data. We first exemplify things by considering the linear constant coefficient case, $f(q) = Aq$, with A defined in (2.3).

The vector q may be decomposed

$$q = P^0 q + P^+ q + P^- q$$

as defined in Section II. It is easy to see that boundary conditions must be of the form

$$P^+ q = P^+ D P^- q + g|_{x=0}, \tag{3.1}$$

where D is a matrix and $g = P^+ g$, a vector. We take them both to be constant, for simplicity only.

The initial-boundary value Riemann problem is defined by solving

$$q_t + A q_x = 0$$

for $x, t \geqslant 0$, with $q(x, 0) \equiv q^R$, a constant, and with boundary data (2.1). This is easily done using the method of characteritics. For our difference schemes we shall need to compute only the resulting boundary values

$$q(0, t) = (P^0 + P^-) \, q^R + P^+ (D P^- q^R + g)$$

and the flux at the boundary:

$$Aq(0, t) = P^- A q^R + P^+ A (D P^- q^R + g). \tag{3.2}$$

To solve this problem approximately, it is convenient to shift our lattice. Adjacent to the boundary begin with $\Omega_{1/2,n} = \{x \mid 0 \leqslant x \leqslant \Delta x, \; t^n \leqslant t < t^{n+1}\}$, and in general

consider $\Omega_{j+1/2,n}$ for j, n nonnegative integers. For all boxes except those adjacent to the boundary we solve the Riemann *initial* value problem. For $q_{1/2}^{n+1}$, we solve the Riemann *initial boundary* value problem.

Thus, Godunov's scheme with this boundary treatment is given by (2.4) for $j = \nu + \frac{1}{2}$, $\nu = 1, 2, \ldots$, and by

$$q_{1/2}^{n+1} = q_{1/2}^{n} - \lambda[P^{+}A(q_{1/2}^{n} - DP^{-}q_{1/2}^{n} - g) + P^{-}A(q_{3/2}^{n} - q_{1/2}^{n})] \tag{3.3}$$

at the boundary.

The full boundary values are also obtained,

$$q_{0}^{n+1} = (P^{0} + P^{-})\, q_{1/2}^{n} + P^{+}(PD^{-}q_{1/2}^{n} + g), \tag{3.4}$$

and these values are taken on at $x = 0$ for all t with $t^{n} < t \leqslant t^{n+1}$.

We now extend this boundary algorithm to the nonlinear problem. We shall do this in sufficient generality to include Euler's equations in higher dimensions with passive tangential variables. This system has a multiple eigenvalue, and may have a characteristic (solid wall) boundary.

We consider first the strictly hyperbolic noncharacteristic boundary case, which means that the eigenvalues satisfy $\lambda_1 < \lambda_2 < \cdots < \lambda_d$, and, at the boundary, there is an index k for which $\lambda_k < 0 < \lambda_{k+1}$. We may write the boundary operator as

$$B(q)_{x=0} = 0, \tag{3.5}$$

where B is $d - k$ vector valued function.

If each j field, for $j \geqslant k + 1$, is either linearly degenerate, or genuinely nonlinear, we may use Lax's construction, [11], to connect the constant state $q_{1/2}$ to physically correct constant left states q_0, using only $k + 1, \ldots, d$ waves. This gives us a $d - k$ parameter family of solutions $q_0(\varepsilon_{k+1}, \ldots, \varepsilon_d)$, whose differential at $\varepsilon_{k+1} = \cdots = \varepsilon_d = 0$ is $[-r_{k+1}(q_{1/2}), \ldots, -r_d(q_{1/2})]$. We must solve (3.5) with $q = q_0(\varepsilon_{k+1}, \ldots, \varepsilon_d)$ for some set of the ε_i.

The mapping $B(q(\varepsilon_{k+1}, \ldots, \varepsilon_d))$ is a locally one-to-one mapping of R^{d-k} into itself, if the solvability condition

$$\det[\nabla_q B \cdot [r_{k+1}(q_{1/2}), \ldots, r_d(q_{1/2})]] \neq 0 \tag{3.6}$$

is satisfied. This is precisely the nonlinear generalization of the rule for selecting boundary conditions in (3.1) above. The Riemann initial-boundary value problem, may now be solved, at least in the small (i.e., in some neighborhood of a solution to (3.5)).

Thus Godunov's scheme will be given by (2.2) for $j = \nu + \frac{1}{2}$, with ν any positive integer, and by (2.2) for $j = \frac{1}{2}$, where the boundary value q_0 is obtained as above.

For Osher's method, the $q - k$ parameter family is obtained, by first solving

$$\dot{q} = r_{k+1}(q), \qquad q(0) = q_{1/2}$$

and obtaining $q(\varepsilon_{k+1})$. We then use this as initial data, solving $\dot{q} = r_{k+\gamma}(q)$, etc., arriving at $q(\varepsilon_{k+1},..., \varepsilon_d)$. Finally, we solve (3.5), which is again possible in the small, given (3.6) above. Osher's algorithm is then defined in the usual way, except at $j = \frac{1}{2}$, where f_0 is defined by (2.8), with the integral taken along the truncated path Γ^0.

Next we consider eigenvalues of constant multiplicity. Suppose $\lambda_{k-1} < \lambda_k \equiv \lambda_{k+1} \equiv \lambda_{k+\gamma-1} < \lambda_{k+\gamma}$. We require that there be γ linearly independent eigenvectors, $r_k,..., r_{k+\gamma-1}$, and that this entire field be linearly degenerate. This means that $\nabla_q \lambda_k$ is orthogonal to the linear span of $r_k,..., r_{k+\gamma-1}$.

Lax's construction can be easily extended to include such fields. The eigenvalues $\lambda_k(q)$ are constant along solutions of $\dot{q} = r_{k+\mu}$, $\mu = 0, 1,..., \gamma - 1$. Thus the right waves corresponding to this field give us a smooth γ parameter family of contact discontinuities $q(\varepsilon_k, \varepsilon_{k+1},..., \varepsilon_{k+\gamma-1})$, which is independent of the choice of basis $r_k,..., r_{k+\gamma-1}$. Each solution has a discontinuity moving with speed $\lambda_k(q)$, independent of $\varepsilon_k,..., \varepsilon_{k+\gamma-1}$. The full Riemann problem may be solved, and Godunov's scheme for the Cauchy problem may be obtained for problems having degenerate fields of this type.

For Osher's method, we see that the path of integration in (2.8) may be obtained in the usual fashion. Moreover, if we define $\Gamma^j_{k,...,k+\gamma-1}$ to be the union of subpaths corresponding to this full field, then the quantity

$$\int_{\Gamma^j_{k,...,k+\gamma-1}} |\partial f(q)|\, dq = \sum_{\mu=0}^{\gamma-1} \int_{\Gamma^j_{k+\mu}} |\partial f(q)|\, dq$$

is easily seen to be independent of the choice of $r_k,..., r_{k+\gamma-1}$. In fact $\int_{q^\beta}^{q^\mu} |\partial f(q)|\, dq$ is path independent, if the path always satisfies $\dot{q} = r_{k+\mu}(q)$, for $0 \leqslant \mu \leqslant \gamma - 1$. This follows from (2.10).

Thus, Osher's scheme for the Cauchy problem may be constructed in the usual fashion for this problem.

If the initial-boundary value problem is noncharacteristic (no λ_j vanishes at the boundary), the procedure at the boundary for both Godunov's and Osher's scheme is the same as that in the noncharacteristic, strictly hyperbolic case, described above.

If, on the other hand, the boundary condition is such as to force the boundary, $x = 0$, to be characteristic, we require that the eigenvalue or eigenvalues vanishing there satisfy the constant multiplicity, linearly degenerate, hypothesis. Thus, we may arrange the eigenvalues in nondecreasing order, with $\lambda_k = 0 < \lambda_{k+1}$ at $x = 0$, and if several eigenvalues vanish there, we require that they all be linearly degenerate. The boundary operator is again written as (3.5), and the initial boundary value problem may be solved, as in the previous case.

Both Godunov's and Osher's schemes now lead to boundary approximations, as in the noncharacteristic case.

The Godunov and Osher algorithms given in Section II for the Cauchy problem, and in Section III for the boundary conditions, are globally defined for Euler equations as long as cavitation does not occur, i.e., as long as the density stays positive. In the use of Godunov's method, cavitation in the solution of Riemann's

problem indicates a genuine physical cavitation. In Osher's approximate Riemann solution, cavitation occurs when the quantity in the numerator of (4.11a) below, turns negative. So far, this has not happened, even for the flows calculated at very high Mach numbers described in Section VI, and elsewhere [3, 19].

For Godunov's scheme with this boundary treatment, it is easily seen that the entropy inequality is valid up to the boundary. Under certain circumstances this fact yields a useful a priori estimate. For both methods, we can show that limit solutions are weak solutions satisfying the boundary conditions in the sense of [13], and that they also satisfy the entropy inequality up to the boundary. This will be discussed in future work.

We do make the following remarks:

REMARK 3.1. Suppose in Osher's method at the boundary we have $\lambda_\gamma(q) \geqslant 0$ on all the corresponding subpaths connecting $q^n_{1/2}$ to q^n_0. Then we have an exact, up to the boundary, conservation law:

$$\frac{1}{\Delta t}\sum_{j=1}^{\infty}(q^{n+1}_{j-1/2}-q^n_{j-1/2})\,\Delta x = f(q^n_0). \tag{3.7}$$

In particular, this is true if $(q^n_{j-1/2}-q^n_0)$ is sufficiently small.

Proof. The explicit numerical algorithm may be written as

$$q^{n+1}_{j-1/2}-q^n_{j-1/2} = -\frac{\Delta t}{2\,\Delta x}\Delta_-\left[f(q^n_{j+1/2})+f(q^n_{j-1/2})-\int_{q^n_{j-1/2}}^{q^n_{j+1/2}}|\partial f(w)|\,dw\right]$$

for $j=1, 2,\ldots$, where we abuse notation, and define $q^n_{-1/2}=q^n_0$, the boundary value.

We multiply by $\Delta x/\Delta t$ and sum from 1 to ∞, arriving at

$$\frac{1}{\Delta t}\sum_{j=1}^{\infty}(q^{n+1}_{j-1/2}-q^n_{j-1/2})\,\Delta x = \frac{1}{2}\left[f(q^n_{1/2})+f(q^n_0)-\int_{q^n_0}^{q^n_{1/2}}|\partial f(w)|\,dw\right].$$

The result follows, since

$$f(q^n_{1/2})-f(q^n_0)=\int_{q^n_0}^{q^n_{1/2}}|\partial f(w)|\,dw=\int_{q^n_0}^{q^n_{1/2}}(\partial f(w))\,dw$$

because our hypothesis guarantees that $\partial f(w)=|\partial f(w)|$ on this path of integration.

REMARK 3.2. The same result is always valid for Godunov's method up to the boundary.

The proof is trivial since

$$\frac{q^{n+1}_{j-1/2}-q^n_{j-1/2}}{\Delta t} = -\left(\frac{f(q^n_j)-f(q^n_{j-1})}{\Delta x}\right)$$

for $j = 1, 2, \ldots$, for q_j^n the solution of the initial or initial-boundary value Riemann problem.

IV. Euler's Equations in General Geometries

Next we turn to the formulation of Osher's scheme in general geometries, with emphasis on the Euler equations. The equivalence of this representation for Godunov's method was presented by Godunov *et al.* in [23].

We begin with a general hyperbolic system of conservation laws in three space dimensions

$$q_t + E(q)_x + F(q)_y + G(q)_z = 0. \tag{4.1}$$

We now change variables in a smooth one to one fashion:

$$\tau = t, \qquad \xi = \xi(x, y, z, t), \qquad \eta = \eta(x, y, z, t), \qquad \zeta = \zeta(x, y, z, t).$$

The equations become

$$\begin{aligned} &q_\tau + \xi_t q_\xi + \xi_x E_\xi + \xi_y F_\xi + \xi_z G_\xi + \eta_t q_\eta + \eta_x E_\eta + \eta_y F_\eta + \eta_z G_\eta \\ &\quad + \zeta_t q_\zeta + \zeta_x E_\zeta + \zeta_y F_\zeta + \zeta_z G_\zeta = 0. \end{aligned} \tag{4.2}$$

We define the Jacobian matrix $\partial E = A$, $\partial F = B$, $\partial G = C$ and assume that all real linear combinations $\alpha A + \beta B + \gamma C$ have eigenvalues and eigenvectors satisfying the hypotheses of the previous section.

We consider the three-dimensional analogue of $\Omega_{j,n}$,

$$\begin{aligned} \Omega_{j,k,l,n} &= \{\xi, \eta, \zeta, t \mid \xi_{j-1/2} \leqslant \xi < \xi_{j+1/2}, \eta_{k-1/2} \leqslant \eta < \eta_{k+1/2}, \\ &\qquad \zeta_{l-1/2} \leqslant \zeta < \zeta_{l+1/2}, t^n \leqslant t < t^{n+1}\} \\ &= \mathscr{I}_j \times \mathscr{I}_k \times \mathscr{I}_l \times \mathscr{T}^n, \end{aligned}$$

with $\xi_j = j\,\Delta\xi$, $\eta_k = k\,\Delta\eta$, $\zeta_l = l\,\Delta\zeta$, $t^n = n\,\Delta t$, as in Section II.

We first approximate the ξ derivative in (4.2), using a frozen coefficient version of the Osher scheme. We drop the k, l, and n sub- and superscripts,

$$\begin{aligned} &\xi_t q_\xi + \xi_x E_\xi + \xi_y F_\xi + \xi_z G_\xi|_{(\xi_j, \eta_k, \zeta_l)} \\ &\quad \sim \frac{1}{\Delta\xi}\left[\int_{q_{j-1}}^{q_j} ((\xi_x)_j A(q) + (\xi_y)_j B(q) + (\xi_z)_j C(q) + (\xi_t)_j I)^+ \, dq \right. \\ &\quad \left. + \int_{q_j}^{q_{j+1}} ((\xi_x)_j A(q) + (\xi_y)_j B(q) + (\xi_z)_j C(q) + \xi_t)_j I)^- \, dq\right] \end{aligned} \tag{4.3}$$

following (2.14). The usual integration paths are taken, here, and in what follows.

We approximate the η, ζ derivatives in the same manner. For simplicity only, we use explicit one step τ differencing.

It is not obvious that the conclusion of the Lax-Wendroff theorem holds for such an approximation, i.e., that bounded almost everywhere limits, as the mesh spacing goes to zero, are indeed weak solutions. This will be proven in the Appendix, Theorem A.1.

In addition, this differencing has the following properties.

(a) Constant states are solutions of the approximation based on (4.3).

(b) One-dimensional steady (i.e., η, ζ, τ independent) solutions, are resolved over two points, as in the cartesian coordinate case.

(c) The Jacobian of the mapping is never used in the calculation.

For the one-dimensional cartesian case, (2.14) may be rewritten as

$$f_{j+1/2} - f_{j-1/2} = \Delta_- \left[f(q_{j+1}) - \int_{q_j}^{q_{j+1}} (\partial f)^+ \, dq \right], \tag{4.4}$$

thereby reducing the required programming by almost a factor of $\frac{1}{2}$.

The approximation using (4.3) will not allow this reduction. Thus following the "variable coefficient" conservation upwind algorithm of Abrahamsson and Osher [1], we have the approximation

$$\begin{aligned} &\xi_t q_\xi + \xi_x E_\xi + \xi_y F_\xi + \xi_z G_\xi \big|_{(\xi_j, \eta_k, \zeta_l)} \qquad (4.5) \\ &\sim \frac{1}{\Delta\xi} \left[\int_{q_{j-1}}^{q_j} ((\xi_x)_{j-1/2} A(q) + (\xi_y)_{j-1/2} B(q) + (\xi_z)_{j-1/2} C(q) + (\xi_t)_{j-1/2} I)^+ \, dq \right. \\ &\quad \left. + \int_{q_j}^{q_{j+1}} ((\xi_x)_{j+1/2} A(q) + (\xi_y)_{j+1/2} B(q) + (\xi_z)_{j+1/2} C(q) + (\xi_t)_{j+1/2} I)^- \, dq \right] \\ &= \frac{1}{\Delta\xi} \left[(\xi_x)_{j+1/2} \Delta_- E(q_{j+1}) + (\xi_y)_{j+1/2} \Delta_- F(q_{j+1}) + (\xi_z)_{j+1/2} \Delta_- G(q_{j+1}) \right. \\ &\quad - \Delta_- \int_{q_j}^{q_{j+1}} ((\xi_x)_{j+1/2} A(q) + (\xi_y)_{j+1/2} B(q) + (\xi_z)_{j+1/2} C(q) \\ &\quad \left. + (\xi_t)_{j+1/2} I)^+ \, dq \right]. \end{aligned}$$

This approximation will lead to a method which satisfies the conclusion of the Lax–Wendroff theorem, as shown in the Appendix. Moreover, properties (a) and (c) are valid, as is the following:

(d) The simplification in programming obtained in (4.4) is valid here.

So far we have not used the following property of Euler's equations pointed out in [20] and elsewhere: The flux functions $E(q)$, $F(q)$, and $G(q)$ are homogeneous of

degree one, as funcitons of q, and hence the matrices $A(q)$, $B(q)$, and $C(q)$ are homogeneous of degree zero. Let $J(\xi, \eta, \zeta, \tau)$ be the Jacobian of the transformation, i.e.,

$$J = \frac{\partial(\xi, \eta, \zeta, \tau)}{\partial(x, y, z, t)} = \det \begin{bmatrix} \xi_x & \xi_y & \xi_z & \xi_t \\ \eta_x & \eta_y & \eta_z & \eta_t \\ \zeta_x & \zeta_y & \zeta_z & \zeta_t \\ 0 & 0 & 0 & 1 \end{bmatrix} = \det \begin{bmatrix} \xi_x & \xi_y & \xi_z \\ \eta_x & \eta_y & \eta_z \\ \zeta_x & \zeta_y & \zeta_z \end{bmatrix}.$$

Then we may rewrite Euler's equation in "homogeneous" conservation form

$$\begin{aligned} &\left(\frac{q}{J}\right)_\tau + \left(\xi_t \left(\frac{q}{J}\right) + \xi_x E\left(\frac{q}{J}\right) + \xi_y F\left(\frac{q}{J}\right) + \xi_z G\left(\frac{q}{J}\right)\right)_\xi \\ &\quad + \left(\eta_t \left(\frac{q}{J}\right) + \eta_x E\left(\frac{q}{J}\right) + \eta_y F\left(\frac{q}{J}\right) + \eta_z G\left(\frac{q}{J}\right)\right)_\eta \\ &\quad + \left(\zeta_t \left(\frac{q}{J}\right) + \zeta_x E\left(\frac{q}{J}\right) + \zeta_y F\left(\frac{q}{J}\right) + \zeta_z G\left(\frac{q}{J}\right)\right)_\zeta = 0. \end{aligned} \tag{4.6}$$

The ξ derivative is approximated as

$$\begin{aligned} &\left(\xi_t \left(\frac{q}{J}\right) + \xi_x E\left(\frac{q}{J}\right) + \xi_y F\left(\frac{q}{J}\right) + \xi_z G\left(\frac{q}{J}\right)\right)_j \Bigg|_{\xi_j, \eta_k, \zeta_l} \\ &\quad \sim \frac{1}{\Delta\xi}\left[\int_{(q/J)_{j-1}}^{(q/J)_j} [(\xi_x)_{j-1/2} A(q) + (\xi_y)_{j-1/2} B(q) + (\xi_z)_{j-1/2} C(q) \right. \\ &\qquad \left. + (\xi_t)_{j-1/2} I]^+ \, dq \right. \\ &\qquad + \int_{(q/J)_j}^{(q/J)_{j+1}} [(\xi_x)_{j+1/2} A(q) + (\xi_y)_{j+1/2} B(q) + (\xi_z)_{j+1/2} C(q) \\ &\qquad + (\xi_t)_{j+1/2} I]^- \, dq \\ &\qquad + (\Delta_-(\xi_x)_{j+1/2}) E\left(\left(\frac{q}{J}\right)_j\right) + (\Delta_-(\xi_y)_{j+1/2}) F\left(\left(\frac{q}{J}\right)_j\right) + (\Delta_-(\xi_z)_{j+1/2}) G\left(\left(\frac{q}{J}\right)_j\right) \\ &\qquad \left. + (\Delta_-(\xi_t)_{j+1/2})\left(\frac{q}{J}\right)_j\right] \\ &\quad = \frac{1}{\Delta\xi}\left[(\xi_x)_{j+1/2} \Delta_- E\left(\left(\frac{q}{J}\right)_{j+1}\right) + (\xi_y)_{j+1/2} \Delta_- F\left(\left(\frac{q}{J}\right)_{j+1}\right)\right. \\ &\qquad \left. + (\xi_z)_{j+1/2} \Delta_- G\left(\left(\frac{q}{J}\right)_{j+1}\right) + (\xi_t)_{j+1/2} \Delta_-\left(\frac{q}{J}\right)_{j+1}\right. \end{aligned} \tag{4.7}$$

$$
\begin{aligned}
-\Delta_- \Bigg(\int_{(q/J)_j}^{(q/J)_{j+1}} & [(\xi_x)_{j+1/2} A(q) + (\xi_y)_{j+1/2} B(q) + (\xi_z)_{j+1/2} C(q) \\
& + (\xi_t)_{j+1/2} I]^+ \, dq \Bigg) \\
& + (\Delta_-(\xi_x)_{j+1/2}) E\left(\left(\frac{q}{J}\right)_j\right) + (\Delta_-(\xi_y)_{j+1/2}) F\left(\left(\frac{q}{J}\right)_j\right) + (\Delta_-(\xi_z)_{j+1/2}) G\left(\left(\frac{q}{J}\right)_j\right) \\
& + (\Delta_-(\xi_t)_{j+1/2}) \left(\frac{q}{J}\right)_j \Bigg].
\end{aligned}
$$

Limit solutions will again be shown to be weak solutions in the appendix.

Properties (b) and (d) are valid (see [1] for the verification of (b)). However, properties (a) and (c) are not. It is not clear whether this method is ever superior to either of the other two, but it does use the homogeneity property in an intriguing manner.

Any of these three methods may be easily used for Euler's equations of compressible gas dynamics, because the eigenvalues, eigenvectors, and in particular, the Riemann invariants for the matrices

$$\xi_t I + \xi_x A(q) + \xi_y B(q) + \xi_z C(q)$$

are easily tabulated in this case.

Euler's equations are

$$
\begin{pmatrix} \rho \\ \rho u \\ \rho v \\ \rho w \\ e \end{pmatrix}_t + \begin{pmatrix} \rho u \\ \rho u^2 + p \\ \rho uv \\ \rho uw \\ u(e+p) \end{pmatrix}_x + \begin{pmatrix} \rho v \\ \rho uv \\ \rho u^2 + p \\ \rho vw \\ v(e+p) \end{pmatrix}_y + \begin{pmatrix} \rho w \\ \rho uw \\ \rho vw \\ \rho w^2 + p \\ w(e+p) \end{pmatrix}_z = \begin{pmatrix} 0 \\ 0 \\ 0 \\ 0 \\ 0 \end{pmatrix}. \tag{4.8}
$$

Here ρ is density, u, v, w are the velocity components, e is the internal energy, p is the pressure defined by $p = (\gamma - 1)(e - (\rho(u^2 + v^2 + w^2)/2))$, the local sound speed is $c = \sqrt{\gamma p/\rho}$, the entropy S is defined by $h(S) = p/\rho^\gamma$, for h some monotone function, and finally, γ is a constant with $\gamma \approx 1.4$ for air.

Thus

$$
\xi_x E + \xi_y F + \xi_z G + \xi_t q = \begin{pmatrix} m\rho\hat{u} \\ m(\rho u)\hat{u} + p\xi_x \\ m(\rho v)\hat{u} + p\xi_y \\ m(\rho w)\hat{u} + p\xi_z \\ m\left(p\dfrac{\gamma}{\gamma - 1} + \dfrac{\rho}{2}(u^2 + v^2 + w^2)\right)\hat{u} - p\xi_t \end{pmatrix}, \tag{4.9}
$$

where

$$\hat{u} = \frac{\xi_t + u\xi_x + v\xi_y + w\xi_z}{m}$$

for

$$m = \sqrt{\xi_x^2 + \xi_y^2 + \xi_z^2}.$$

It can be shown that the matrix

$$\xi_x A + \xi_y B + \xi_z C + \xi_t I$$

has eigenvalues $m(\hat{u} - c) < m\hat{u} < m(\hat{u} + c)$, where $m\hat{u}$ has multiplicity three. The eigenvectors corresponding to $m\hat{u}$, span a three-dimensional space. The eigenvalue is linearly degenerate, which means $\nabla_q \hat{u}$ is orthogonal to this space. A second independent function whose gradient has this property is the pressure p. These two functions serve as Riemann invariants for this intermediate field.

The Riemann invariants corresponding to $\lambda_1 = (\hat{u} - c)m$ are the entropy p/ρ^γ, $\hat{u} + (2/(\gamma - 1))c$, and any two independent contravariant velocities, say,

$$\hat{v} = \frac{-u\xi_y + v\xi_x}{m},$$

$$\hat{w} = \frac{-u\xi_z + w\xi_x}{m},$$

where we assume $\xi_x \neq 0$, without loss of generality.

The linear map $u, v, w \to \hat{u}, \hat{v}, \hat{w}$ and its inverse, are defined by

$$m\begin{pmatrix} \hat{u} \\ \hat{v} \\ \hat{w} \end{pmatrix} - \begin{pmatrix} \xi_t \\ 0 \\ 0 \end{pmatrix} = \begin{pmatrix} \xi_x & \xi_y & \xi_z \\ -\xi_y & \xi_x & 0 \\ -\xi_z & 0 & \xi_x \end{pmatrix}\begin{pmatrix} u \\ v \\ w \end{pmatrix}$$

and

$$\begin{pmatrix} u \\ v \\ w \end{pmatrix} = \frac{1}{\xi_x m^2}\begin{pmatrix} \xi_x^2 & -\xi_y\xi_x & -\xi_x\xi_z \\ \xi_y\xi_x & \xi_x^2 + \xi_z^2 & -\xi_y\xi_z \\ \xi_x\xi_z & -\xi_z\xi_y & \xi_x^2 + \xi_y^2 \end{pmatrix}\begin{pmatrix} m\hat{u} - \xi_t \\ m\hat{v} \\ m\hat{w} \end{pmatrix},$$

respectively.

Finally, the Riemann invariants which correspond to $\lambda_5 = (\hat{u} + c)m$ are p/ρ^γ, $\hat{u} - (2/(\gamma - 1))c$, $\hat{v}$, and $\hat{w}$.

The curve Γ^{j-1} is made up of piecewise smooth subcurves and their end points q_j, $q_{j-1/3}$, $q_{j-2/3}$, q_{j-1}. (Actually $q_{j-1/3}$, $q_{j-2/3}$ can be connected by any subcurve in the hypersurface determined by setting $\hat{u}$ and p to be constant.) See Fig. 1 for a schematic representation of this construction for the two-dimensional case.

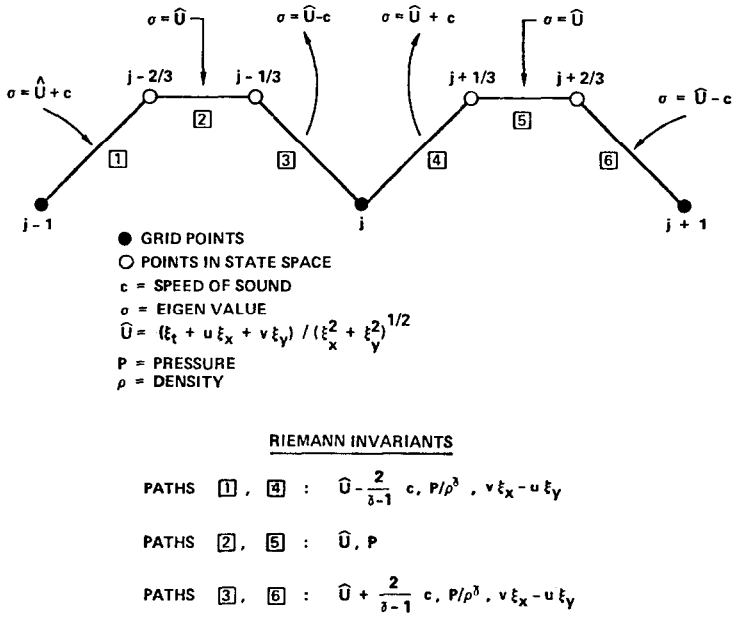

FIG. 1. Schematic representation of Osher scheme.

The points of intersection are found by solving the following set of ten equations in as many unknowns:

$$\text{(a)} \qquad \left(\frac{p}{\rho^\gamma}\right)_{j-1/3} = \left(\frac{p}{\rho^\gamma}\right)_j, \tag{4.10}$$

$$\left(\hat{u} + \frac{2}{\gamma-1}c\right)_{j-1/3} = \left(\hat{u} + \frac{2}{\gamma-1}c\right)_j,$$

$$\hat{v}_{j-1/3} = \hat{v}_j,$$

$$\hat{w}_{j-1/3} = \hat{w}_j,$$

$$\text{(b)} \qquad \hat{u}_{j-2/3} = \hat{u}_{j-1/3},$$

$$p_{j-2/3} = p_{j-1/3},$$

$$\text{(c)} \qquad \left(\frac{p}{\rho^\gamma}\right)_{j-1} = \left(\frac{p}{\rho^\gamma}\right)_{j-2/3},$$

$$\left(\hat{u} - \frac{2}{\gamma-1}c\right)_{j-1} = \left(\hat{u} - \frac{2}{\gamma-1}c\right)_{j-2/3},$$

$$\hat{v}_{j-1} = \hat{v}_{j-2/3},$$

$$\hat{w}_{j-1} = \hat{w}_{j-2/3}.$$

The first four equations determine a curve in I_1^{j-1}, in phase space (R^5) passing through q_j. The last four determine I_5^{j-1} passing through q_{j-1}. The middle two determine a surface of codimension three. The points of intersection are determined by

$$\text{(a)} \quad \rho_{j-1/3}^{(\gamma-1)/2} = \left(\frac{((\gamma-1)/2)(\hat{u}_j - \hat{u}_{j-1}) + c_j + c_{j-1}}{c_j(1 + (p_{j-1}/p_j)^{(1/2\gamma)}(\rho_{j-1}/\rho_j)^{(-1/2)})} \right) \rho_j^{(\gamma-1)/2}, \tag{4.11}$$

$$\text{(b)} \quad \rho_{j-2/3}^{(\gamma-1)/2} = \left(\frac{((\gamma-1)/2)(\hat{u}_j - \hat{u}_{j-1}) + c_j + c_{j-1}}{c_{j-1}(1 + (p_j/p_{j-1})^{(1/2\gamma)}(\rho_j/\rho_{j-1})^{(-1/2)})} \right) \rho_{j-1}^{(\gamma-1)/2},$$

$$\text{(c)} \quad p_{j-2/3} = p_{j-1/3} = p_{j-1} \left(\frac{\rho_{j-1}}{\rho_{j-2/3}} \right)^{-\gamma},$$

$$\text{(d)} \quad \hat{u}_{j-2/3} = \hat{u}_{j-1/3} = \hat{u}_{j-1} - \frac{2}{\gamma-1} \left(c_{j-1} - \sqrt{\frac{\gamma p_{j-2/3}}{\rho_{j-2/3}}} \right),$$

$$\text{(e)} \quad \hat{w}_{j-2/3} = \hat{w}_{j-1}, \qquad \hat{w}_{j-1/3} = \hat{w}_j,$$

$$\text{(f)} \quad \hat{v}_{j-2/3} = \hat{v}_{j-1}, \qquad \hat{v}_{j-1/3} = \hat{v}_j.$$

For the first and last genuinely nonlinear fields, we calculate the sonic points $\mathbf{q}_{j-1/3}$, $\mathbf{q}_{j-2/3}$:

$$\text{(a)} \quad (\boldsymbol{\rho}_{j-1/3})^{(\gamma-1)/2} = \frac{((\gamma-1)/(\gamma+1))(\hat{u}_j + (2/(\gamma-1))\, c_j)}{c_j} (\rho_j)^{(\gamma-1)/2}, \tag{4.12}$$

$$\text{(b)} \quad \mathbf{p}_{j-1/3} = p_j \left(\frac{\boldsymbol{\rho}_{j-1/3}}{\rho_j} \right)^{\gamma},$$

$$\text{(c)} \quad \hat{\mathbf{u}}_{j-1/3} = \hat{u}_j + \frac{2}{\gamma-1} c_j \left(1 - \left(\frac{\boldsymbol{\rho}_{j-1/3}}{\rho_j} \right)^{(\gamma-1)/2} \right),$$

$$\text{(d)} \quad (\boldsymbol{\rho}_{j-2/3})^{(\gamma-1)/2} = \frac{((\gamma-1)/(\gamma+1)(2/(\gamma-1))\, c_{j-1} - \hat{u}_j)}{c_{j-1}} (\rho_{j-1})^{(\gamma-1)/2},$$

$$\text{(e)} \quad \mathbf{p}_{j-2/3} = p_{j-1} \left(\frac{\rho_{j-2/3}}{\rho_{j-1}} \right)^{\gamma},$$

$$\text{(f)} \quad \hat{\mathbf{u}}_{j-2/3} = \hat{u}_{j-1} - \frac{2}{\gamma-1} c_{j-1} \left(1 - \left(\frac{\boldsymbol{\rho}_{j-2/3}}{\rho_{j-1}} \right)^{(\gamma-1)/2} \right),$$

$$\text{(g)} \quad \hat{\mathbf{v}}_{j-2/3} = \hat{v}_{j-1}, \qquad \hat{\mathbf{v}}_{j-1/3} = \hat{v}_j,$$

$$\text{(h)} \quad \hat{\mathbf{w}}_{j-2/3} = \hat{w}_{j-1}, \qquad \hat{\mathbf{w}}_{j-1/3} = \hat{w}_j.$$

We may now compute all the integral (4.3), (4.5), or (4.7). For (4.3), the values of

ξ_x, ξ_y, ξ_z, and ξ_t are all fixed at (ξ_j, η_k, ζ_l). As mentioned above, the linearly degenerate contribution simplifies:

$$\text{(a)} \quad \int_{q_{j-2/3}}^{q_{j-1/3}} (\xi_x A(q) + \xi_y B(q) + \xi_z C(q) + \xi_t I)^+ \, dq$$

$$= \xi_x E + \xi_y F + \xi_z G + \xi_t q \Big]_{q_{j-2/3}}^{q_{j-1/3}} \quad \text{if} \quad \hat{u}_{j-2/3} > 0$$

$$= 0 \quad \text{if} \quad \hat{u}_{j-2/3} \leqslant 0, \tag{4.13}$$

$$\text{(b)} \quad \int_{q_{j+1/3}}^{q_{j+2/3}} (\xi_x A(q) + \xi_t B(q) + \xi_z C(q) + \xi_t I)^- \, dq$$

$$= 0 \quad \text{if} \quad \hat{u}_{j+1/3} > 0$$

$$= \xi_x E + \xi_y F + \xi_z G + \xi_t q \Big]_{q_{j+1/3}}^{q_{j+2/3}} \quad \text{if} \quad \hat{u}_{j+1/3} \leqslant 0.$$

The genuinely nonlinear contributions are

$$\text{(a)} \quad \int_{q_{j-1}}^{q_{j-2/3}} (\xi_x A(q) + \xi_y B(q) + \xi_z C(q) + \xi_t I)^+ \, dq \tag{4.14}$$

$$= \xi_x E(q) + \xi_y F(q) + \xi_z G(q) + \xi_t q \begin{cases} q_{j-2/3} & \text{if} \quad \hat{u}_{j-2/3} + c_{j-2/3} > 0 \\ \mathbf{q}_{j-2/3} & \text{if} \quad \hat{u}_{j-2/3} + c_{j-2/3} \leqslant 0 \\ q_{j-1} & \text{if} \quad \hat{u}_{j-1} + c_{j-1} > 0 \\ \mathbf{q}_{j-2/3} & \text{if} \quad \hat{u}_{j-1} + c_{j-1} \leqslant 0, \end{cases}$$

$$\text{(b)} \quad \int_{q_j}^{q_{j+1/3}} (\xi_x A(q) + \xi_y B(q) + \xi_z C(q) + \xi_t I)^- \, dq$$

$$= \xi_x E(q) + \xi_y F(q) + \xi_z G(q) + \xi_t q \begin{cases} q_{j+1/3} & \text{if} \quad \hat{u}_{j+1/3} + c_{j+1/3} < 0 \\ \mathbf{q}_{j+1/3} & \text{if} \quad \hat{u}_{j+1/3} + c_{j+1/3} \geqslant 0 \\ q_j & \text{if} \quad \hat{u}_j + c_j < 0 \\ \mathbf{q}_{j+1/3} & \text{if} \quad \hat{u}_j + c_j \geqslant 0. \end{cases}$$

Finally

$$\text{(a)} \quad \int_{q_{j-1/3}}^{q_j} (\xi_x A(q) + \xi_y B(q) + \xi_z C(q) + \xi_t I)^+ \, dq$$

$$= \xi_x E(q) + \xi_y F(q) + \xi_z G(q) + \xi_t q \begin{cases} q_j & \text{if} \quad \hat{u}_j - c_j > 0 \\ \mathbf{q}_{j-1/3} & \text{if} \quad \hat{u}_j - c_j \leqslant 0 \\ q_{j-1/3} & \text{if} \quad \hat{u}_{j-1/3} - c_{j-1/3} > 0 \\ \mathbf{q}_{j-1/3} & \text{if} \quad \hat{u}_{j-1/3} - c_{j-1/3} \leqslant 0, \end{cases} \tag{4.15}$$

(b) $$\int_{q_{j+2/3}}^{q_{j+1}} (\xi_x A(q) + \xi_y B(q) + \xi_z C(q) + \xi_t I)^- \, dq$$

$$= \xi_x E(q) + \xi_y F(q) + \xi_z G(z) + \xi_t q \begin{cases} q_{j+1} & \text{if } \hat{u}_{j+1} - c_{j+1} < 0 \\ \mathbf{q}_{j+2/3} & \text{if } \hat{u}_{j+1} - c_{j+1} \geqslant 0 \\ q_{j+2/3} & \text{if } \hat{u}_{j+2/3} - c_{j+2/3} < 0 \\ \mathbf{q}_{j+2/3} & \text{if } \hat{u}_{j+2/3} - c_{j+2/3} \geqslant 0. \end{cases}$$

We add (4.13), (4.14), and (4.15) to obtain the differencing in (4.3).

To obtain the differencing in (4.5), we need only compute the integrals in (4.13a), (4.14a), (4.15a) at $(\xi_{j-1/2}, \eta_k, \zeta_l)$ and $(\xi_{j+1/2}, \eta_k, \zeta_l)$, and then use the formula on the right in (4.5).

For the differencing in (4.7), we use the expression on the right for the grid points $(\xi_{j-1/2}, \eta_k, \zeta_l)$ and $(\xi_{j+1/2}, \eta_k, \zeta_l)$, but the limits of integration are different. This presents no difficulties. We merely replace q by q/J. The components transform via $\rho \to \rho/J$, $e \to e/J$, $p \to p/J$. The remainder of the construction is as above.

We now make some computational remarks. Note that in (4.14a), if $\hat{u} + c \leqslant 0$ at both endpoints, the integral is automatically zero, and the sonic points need not be computed. Similar remarks hold for all the integrals in (4.14) and (4.15). We also note that it is easy to decode u, v, w from the contravariant velocities $\hat{u}, \hat{v}, \hat{w}$.

V. Boundary Conditions for Euler's Equations in General Geometries

We again consider Euler's equation (4.8), transformed to the system (4.2). Our region will be

$$\tau \geqslant 0, \qquad \xi \geqslant 0, \qquad -\infty < \eta, \zeta < \infty.$$

This will be appropriate if we use body fitted coordinates, with $\xi = 0$ as the boundary. For simplicity of exposition only, we omit more general cases which can be treated as long as each boundary corresponds to any of ξ, η, or ζ being constant.

The space time lattice is made up of rectangles:

$$\Omega_{j,k,l,n} = \{(\xi, \eta, \zeta, \tau) \mid (j - \tfrac{1}{2})\Delta\xi \leqslant \xi < (j + \tfrac{1}{2})\Delta\xi, (k - \tfrac{1}{2})\Delta\eta \leqslant \eta < (k + \tfrac{1}{2})\Delta\eta,$$
$$(l - \tfrac{1}{2})\Delta\zeta \leqslant \zeta < (l + \tfrac{1}{2})\Delta\zeta, n\Delta\tau \leqslant \tau < (n + 1)\Delta\tau$$

for $j = \frac{1}{2}, \frac{3}{2}, \frac{5}{2}, \ldots$, $n = 0, 1, 2, \ldots$, and k, l taking on all integral values. See Fig. 2 for an illustration of the boundary point discretization.

We suppress the k, l, and n indices in what follows.

We begin with the physical solid wall (characteristic) boundary condition, $\hat{u} = 0$ at $\xi = 0$. Thus, at the boundary, we have $\lambda_1 = -mc < \lambda_2 = \lambda_3 = \lambda_4 = 0 < \lambda_5 = mc$. According to our analysis in Section III, we can find q_0, the boundary value, by

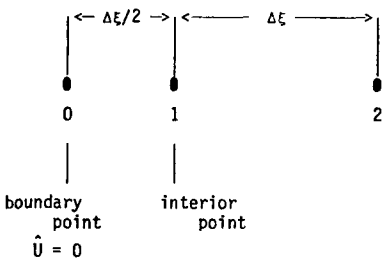

FIG. 2. Boundary point discretization.

connecting $q_{1/2}$ to q_0 on the left, using only a five wave. A simple calculation gives us q_0, defined by

$$(\rho_0)^{(\gamma-1)/2} = \left(\frac{c_{1/2} - ((\gamma-1)/2)\,\hat{u}_{1/2}}{c_{1/2}}\right) \rho_{1/2}^{(\gamma-1)/2}, \tag{5.1}$$

$$\hat{u}_0 = 0,$$

$$\hat{v}_0 = v_{1/2},$$

$$\hat{w}_0 = w_{1/2},$$

$$p_0 = \left(\frac{c_{1/2} - ((\gamma-1)/2)\,\hat{u}_{1/2}}{c_{1/2}}\right) p_{1/2}.$$

We obtain $q_{1/6}$, the sonic point for this five wave:

$$-\hat{\mathbf{u}}_{1/6} = \mathbf{c}_{1/6} = \frac{\gamma-1}{\gamma+1}\left(\frac{2}{\gamma-1}\,c_{1/2} - \hat{u}_{1/6}\right), \tag{5.2}$$

$$\hat{\mathbf{v}}_{1/6} = v_{1/2},$$

$$\hat{\mathbf{w}}_{1/6} = w_{1/2},$$

$$(\boldsymbol{\rho}_{1/6})^{(\gamma-1/2)} = \left(\frac{(2/(\gamma+1))\,c_{1/2} - ((\gamma-1)/(\gamma+1))\,\hat{u}_{1/2}}{c_{1/2}}\right) (\rho_{1/2})^{(\gamma-1)/2}.$$

The approximation of type (4.3) at the point adjacent to the boundary, $j = \frac{1}{2}$, is obtained replacing the + integral in (4.3) by

$$\int_{q_0}^{q_{1/2}} ((\xi_x)_{1/2}\,A(q) + (\xi_y)_{1/2}\,B(q) + (\xi_z)_{1/2}\,C(q) + (\xi_t)_{1/2}\,I)^+\,dq \tag{5.3}$$

$$= (\xi_x)_{1/2}\,E(q) + (\xi_y)_{1/2}\,F(q) + (\xi_z)_{1/2}\,G(q) + (\xi_t)_{1/2}\,qI \Big|_{\substack{q_{1/2} \\ \mathbf{q}_{1/6} \\ q_0}} \quad \begin{array}{ll} \text{if} & \hat{u}_{1/2} + c_{1/2} > 0 \\ \text{if} & \hat{u}_{1/2} + c_{1/2} \leqslant 0 \end{array}$$

For the differencing using (4.5) at $j = \frac{1}{2}$, we do the same with $(\xi_x)_0$, $(\xi_y)_0$, $(\xi_z)_0$, $(\xi_t)_0$ replacing the subscripts $\frac{1}{2}$ above. This approximation should, for this reason, be more accurate than the previous one.

For the approximation based on (4.7) at $j = \frac{1}{2}$, we proceed as in the initial value problem. We replace $\rho \to \rho/J$, $e \to e/J$, $p \to p/J$, and the remaining construction of the + integral is as in the previous case.

Next we consider an open boundary located in the interior of a gas. In this case the normal velocity may not be zero except at isolated points. For supersonic boundaries, all quantities should be specified at inflow points, and no quantities at outflow.

Suppose $\xi = 0$ is a supersonic inflow point. Then all the quantities $\rho, \rho u, \rho v, \rho w$, and e are specified at $\xi = 0$, with $\hat{u} > c$ there. Then we may treat the boundary values as known quantities q_0, and the + integrals in (4.3), (4.5), and (4.7) are computed at $j = \frac{1}{2}$, with the lower limit replaced by, respectively, q_0, q_0, or q_0/J_0.

If $\xi = 0$ is a supersonic outflow point, than no boundary conditions are given there, and $q_0 \equiv q_{1/2}$. Again, the + integrals are treated as above, which gives us a zero contribution in (4.3), (4.5), but which yields

$$\int_{q_{1/2}/J_0}^{q_{1/2}/J_{1/2}} ((\xi_x)_0 A(q) + (\xi_y)_0 B(q) + (\xi_z)_0 C(q) + (\xi_t)_0 I)\, dq,$$

along the usual path, in (4.7).

For subsonic inflow points, $0 < \hat{u} < c$, four boundary conditions must be imposed, while for outflow points, $-c < \hat{u} < 0$, one condition is imposed. Oliger and Sundström [15], have obtained families of boundary conditions for these problems, for which they proved well-posedness of the linearized initial-boundary value problem.

On at outflow boundary, the possible well-posed boundary condition might be to connecting $q_{1/2}$ to q_0 on the left, using only a five wave.

Suppose we prescribe p_0. A simple calculation gives us

$$\rho_0 = \left(\frac{p_0}{p_{1/2}}\right)^{1/\gamma} \rho_{1/2}, \tag{5.4}$$

$$c_0 = \sqrt{\frac{\gamma p_0}{\rho_0}} = c_{1/2} \left(\frac{p_0}{p_{1/2}}\right)^{(\gamma-1)/2\gamma},$$

$$\hat{u}_0 = \hat{u}_{1/2} - \frac{2}{\gamma - 1} c_{1/2} \left(1 - \left(\frac{p_0}{p_{1/2}}\right)^{(\gamma-1)/2\gamma}\right),$$

$$\hat{v}_0 = \hat{v}_{1/2},$$

$$\hat{w}_0 = \hat{w}_{1/2}.$$

If, instead, we prescribe $\hat{u}_0$, we arrive at

$$(\rho_0)^{(\gamma-1)/2} = \left(\frac{(\gamma-1)/2)(\hat{u}_0 - \hat{u}_{1/2}) + c_{1/2}}{c_{1/2}}\right)(\rho_{1/2})^{(\gamma-1)/2}, \tag{5.5}$$

$$p_0 = \left(\frac{((\gamma-1)/2)(\hat{u}_0 - \hat{u}_{1/2}) + c_{1/2}}{c_{1/2}}\right)^{2\gamma/(\gamma-1)} p_{1/2},$$

$$\hat{v}_0 = \hat{v}_{1/2},$$

$$\hat{w}_0 = \hat{w}_{1/2}.$$

The sonic point for either of these five waves is the same as that in (5.2). Thus, the differencing at the boundary is obtained using these boundary values, just as in the solid wall characteristic case.

For subsonic inflow points, we may prescribe $\hat{v}_0, \hat{w}_0, p_0/\rho_0^\gamma$, and one of $\hat{u}_0, \rho_0$, or $\hat{u}_0 + (2/(\gamma-1))c_0$. (Other possibilities are also listed in [15].) We must use a five wave, which gives us the following four equations for the components of $q_{1/6}$:

$$p_{1/6}/(\rho_{1/6})^\gamma = p_0/(\rho_0)^\gamma, \tag{5.6}$$

$$\hat{u}_{1/6} - \frac{2}{\gamma-1} c_{1/6} = \hat{u}_0 - \frac{2}{\gamma-1} c_0,$$

$$\hat{v}_{1/6} = \hat{v}_0,$$

$$\hat{w}_{1/6} = \hat{w}_0.$$

Then we connect $q_{1/6}$ to $q_{1/2}$, via

$$\hat{u}_{1/6} = \hat{u}_{1/2}, \tag{5.7}$$

$$p_{1/6} = p_{1/2}.$$

This, together with the boundary conditions, gives us ten equations in ten unknowns.

We have

$$\rho_{1/6} = (p_{1/2}/p_0)^{1/\gamma}\rho_0.$$

This also determines $c_{1/6}$, and hence $q_{1/6}$.

If we are given ρ_0, then c_0 is known from the boundary conditions, and

$$\hat{u}_0 = \hat{u}_{1/6} - \frac{2}{\gamma-1}(c_{1/6} - c_0).$$

This can be used to determine ρ_0 if $\hat{u}_0$ is given instead.

Finally, given $\hat{u}_0 + (2/(\gamma-1))\,c_0$, we obtain

$$c_0 = \frac{\gamma-1}{4}\left(\hat{u}_0 + \frac{2}{\gamma-1}c_0 - \hat{u}_{1/6} + \frac{2}{\gamma-1}c_{1/6}\right).$$

Since the five wave connects q_0 to $q_{1/6}$, the sonic point $\mathbf{q}_{1/6}$ is found to be

$$-\hat{\mathbf{u}}_{1/6} = \mathbf{c}_{1/6} = \frac{\gamma-1}{\gamma+1}\left(\frac{2}{\gamma-1}c_0 - \hat{u}_0\right), \tag{5.8}$$

$$\hat{\mathbf{w}}_{1/6} = \hat{\mathbf{w}}_0,$$

$$\hat{\mathbf{v}}_{1/6} = \hat{\mathbf{v}}_0,$$

$$\mathbf{p}_{1/6}^{(\gamma-1)/2} = \left(\frac{(2/(\gamma-1))\,c_0 - ((\gamma-1)/(\gamma+1))\,\hat{u}_0}{c_0}\right)\rho_0^{(\gamma-1)/2}.$$

The approximation corresponding to (4.3), at $j = \frac{1}{2}$, is obtained by defining the $+$ integral to be

$$\int_{q_0}^{q_{1/6}} ((\xi_x)_{1/2}A(q) + (\xi_y)_{1/2}B(q) + (\xi_z)_{1/2}C(q) + (\xi_t)I)^+\,dq$$

$$= \chi(\hat{u}_{1/2})\left[(\xi_x)_{1/2}E(q) + (\xi_y)_{1/2}F(q) + (\xi_z)_{1/2}G(q) + (\xi_t)_{1/2}qI\right]\Big|_{q_{1/6}}^{q_{1/2}}$$

$$+ (\xi_x)_{1/2}E(q) + (\xi_y)_{1/2}F(q) + (\xi_z)_{1/2}G(z) + (\xi_t)_{1/2}qI\Big|_{q_0}^{\begin{cases} q_{1/6} & \text{if } \hat{u}_{1/6} + c_{1/6} > 0 \\ \mathbf{q}_{1/6} & \text{if } \hat{u}_{1/6} + c_{1/6} \leqslant 0 \end{cases}}$$

Here $\chi(u) = 1$ if $u \geqslant 0$, $\chi(u) = 0$ if $u < 0$.

The boundary approximations for (5.5) and (5.7) are obtained analogously.

VI. Results

In this section, we consider the application of the theory discussed in Sections III to V to several example problems. We first show results for a one-dimensional shock tube problem with a stationary shock wave. The non-isentropic Euler equations for this case are

$$\begin{pmatrix} \rho \\ \rho u \\ e \end{pmatrix}_t + \begin{pmatrix} \rho u \\ \rho u^2 + p \\ (e+p)u \end{pmatrix}_x = 0. \tag{6.1}$$

Figure 3 shows results for a case with Mach number of 2.0 upstream of the shock.

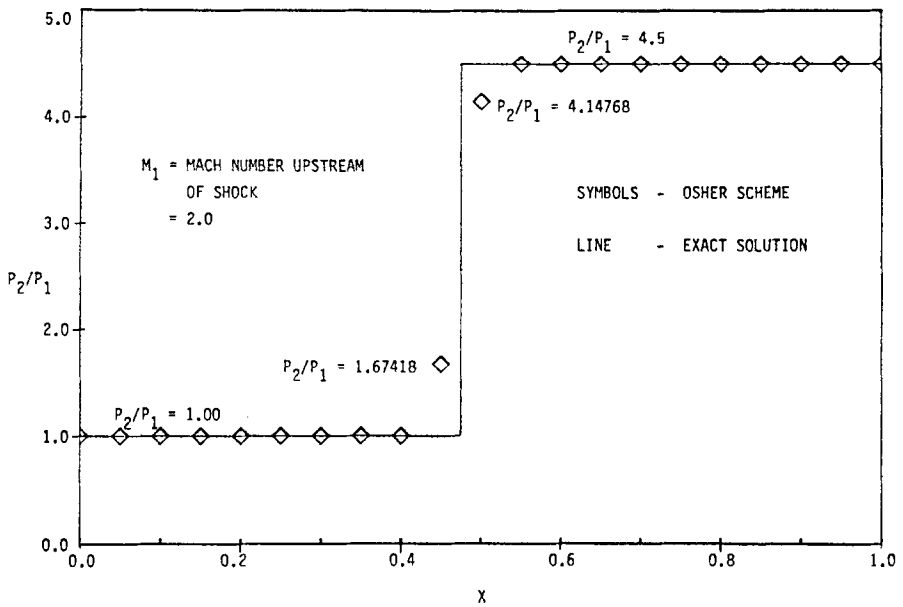

FIG. 3. Comparison of pressure distribution for one-dimensional shock tube problem. Mach number upstream of shock = 2.00.

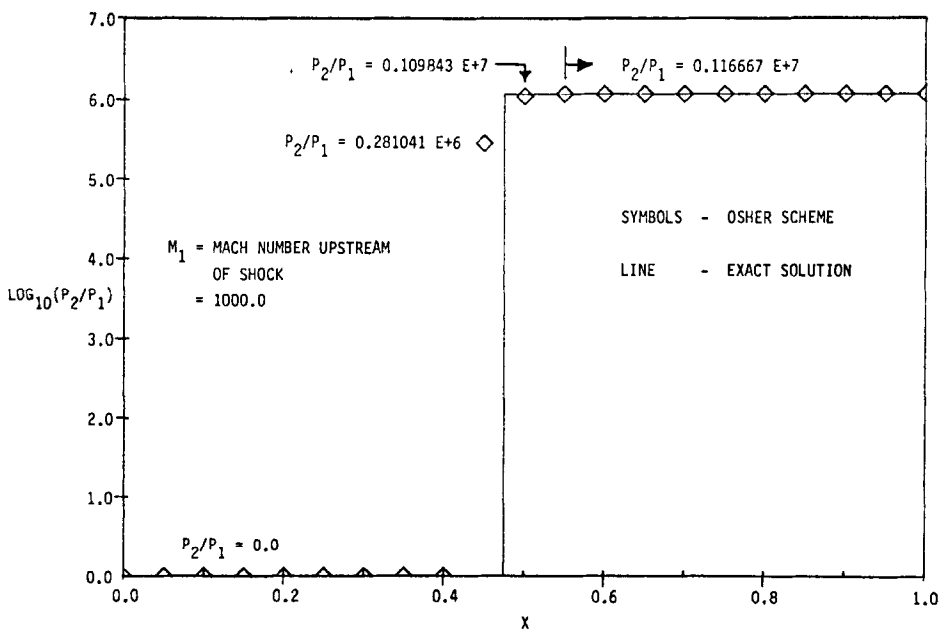

FIG. 4. Comparison of pressure distribution for one-dimensional shock tube problem. Mach number upstream of shock = 1000.0.

The two point shock transition is clearly seen. The points on either side of the shock are precisely equal to the exact solution at these points. Figure 4 shows the same kind of comparison but for an upsteam Mach number of 1000.0. Once again, but for the two transition points, the numerical and exact solutions match perfectly (up to computer precision).

The first example discussed above did not require the use of either the boundary condition treatment covered in Sections III and IV, or arbitrary coordinate transformations. The next example is the quasi-one-dimensional flow through a Laval nozzle. The computational analysis for this case requires the use of a subsonic outflow boundary condition with the pressure specified such that a shock is situated in the middle of the duct. The governing equations may be written as

$$\frac{\partial q}{\partial t} + \frac{\partial E}{\partial x} + \left(\frac{\partial A/\partial x}{A}\right) H = 0. \tag{6.2}$$

The variables q and E are those in Eq. (6.1) and

$$H = \begin{bmatrix} \rho u \\ \rho u^2 \\ (e+p)u \end{bmatrix}$$

while the area of the nozzle varies as a function of x: $(A(x))$. For the particular case considered,

$$A(x) = 0.5 + 0.25x^2. \tag{6.3}$$

A slight modification of the boundary point treatment of Section V is used to adapt the procedure to a grid where the boundary point is located a distance Δx from its interior neighbor. For an inflow supersonic Mach number of 2.0, the numerically obtained pressure distribution is compared with the exact solution in Fig. 5. The agreement is evident, along with the sharp shock transition.

The third example considered is the supersonic flow past a wedge. The wedge surface is laid out aligned with the x axis with the free stream flow inclined to this surface. For negative incidence α, a straight oblique shock attached to the leading edge of the wedge must result, while for positive α, a Prandtl–Meyer expansion fan centered at the leading edge must occur. To solve this problem, we employ an independent variable transformation of the type $\xi = x$ and $\eta = y/x$. The desired solutions are self-similar with respect to ξ and thus variations of q, E, F with respect to ξ are set to zero to reduce the governing equations to one spatial coordinate η. The results presented are for a free stream Mach number of 2.0 and the second form of the algorithm (Eq. (4.5)) is utilized for this and the next examples.

First we compare the numerical and exact solutions for $\alpha = -10.0°$ where the oblique shock is situated at approximately 30° from the wedge surface. Figure 6 shows the agreement for this case. Next we consider $\alpha = +10°$ in Fig. 7. Once again, agreement between the numerical and exact solutions is clearly seen. The good

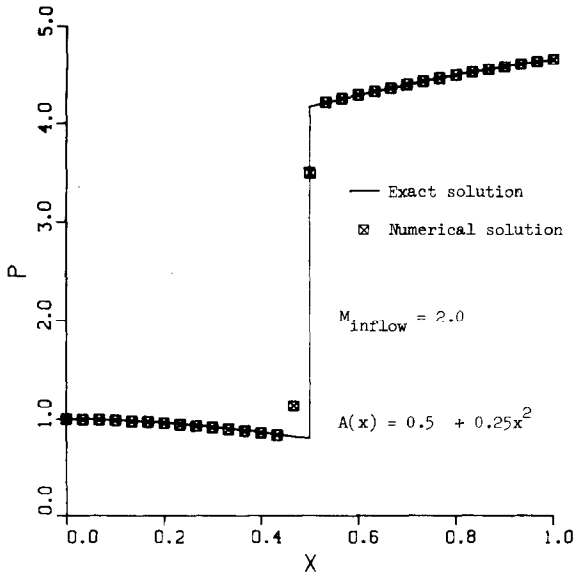

FIG. 5. Flow through quasi-one-dimensional Laval nozzle.

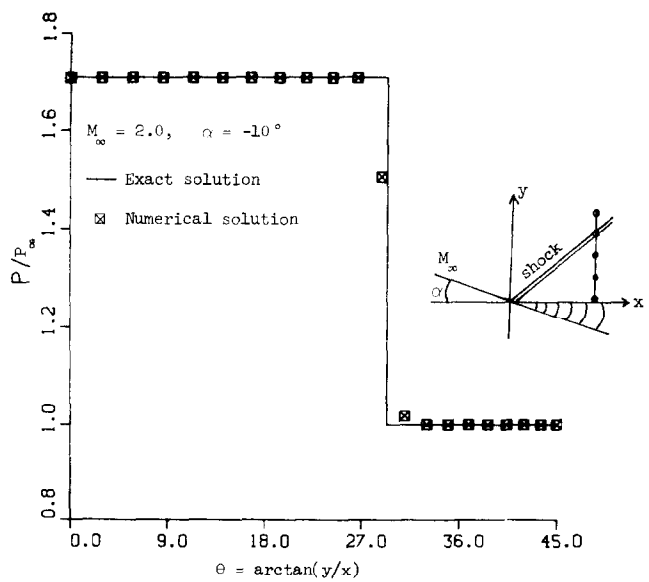

FIG. 6. Wedge in supersonic flow of $M_\infty = 2.0$ and $\alpha = -10°$.

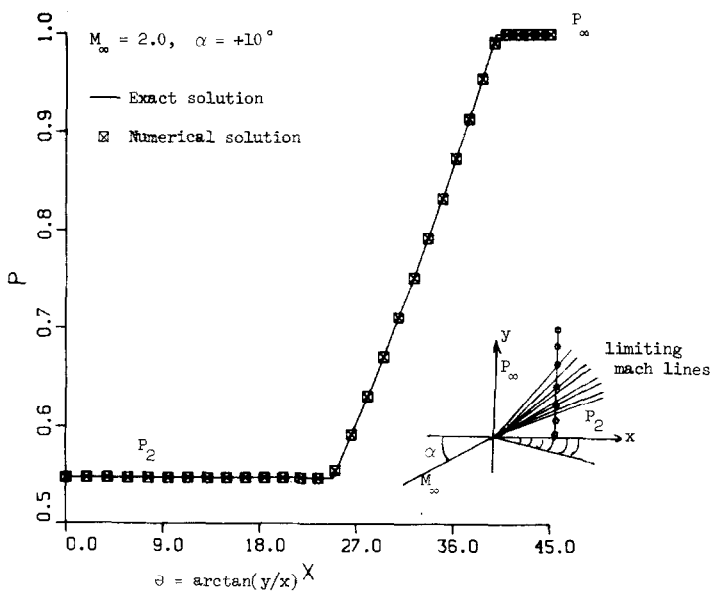

FIG. 7. Wedge in supersonic flow with $M_\infty = 2.0$, $\alpha = +10°$.

behavior of the numerical solution near the points of slope discontinuity in the pressure distribution is also obvious. The absence of any oscillations of smearing offers some proof of the abilities of the numerical method.

Finally, we turn our attention to the two-dimensional flow past a circular cylinder with a free stream Mach number of 8.0. The computational domain was chosen to include the bow shock in its interior. The grid lines were constructed by first choosing an outer boundary shape, drawing radial lines at equiangular increments and drawing the other family of lines to be equally spaced between cylinder and outer boundary. The calculations were begun impulsively by prescribing free stream quantities at all points and in the next step latting the body boundary condition to be fully felt. Convergence from such a start clearly demonstrated the robustness of the numerical procedure.

Contour lines of constant pressure obtained from the numerical results are plotted as solid lines in Fig. 8. The computational grid is also shown in this figure as a superimposed set of dashed lines. The crisp shock transition is clearly evident in this portrayal of results. Like the one-dimensional problems, the shock transition for this case with the grid almost aligned with the shock takes place in two points. In Fig. 9 we show the Mach number contours in increments of 0.2. Here we superimpose with triangular symbols the location of the shock as predicted by a shock "fit" calculation [18]. Good agreement is evident, especially considering the current first order accuracy of our numerical procedure. A comparison of the surface pressure distribution between our results and the shock "fitted" calculations of Lyubimov and Rusanov [18] are shown in Fig. 10. Once again reasonably good agreement is

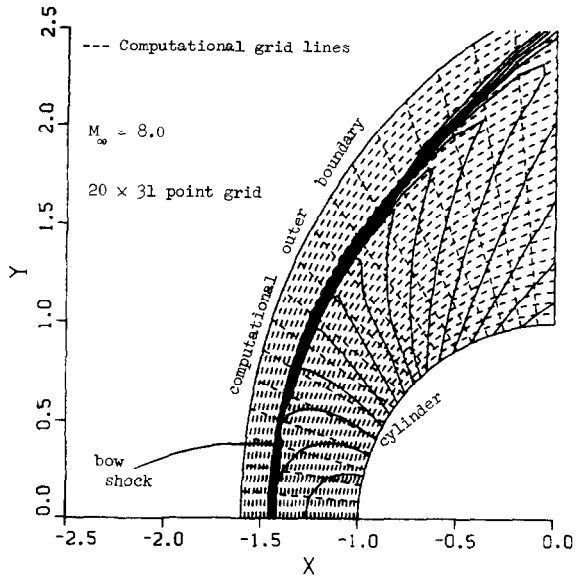

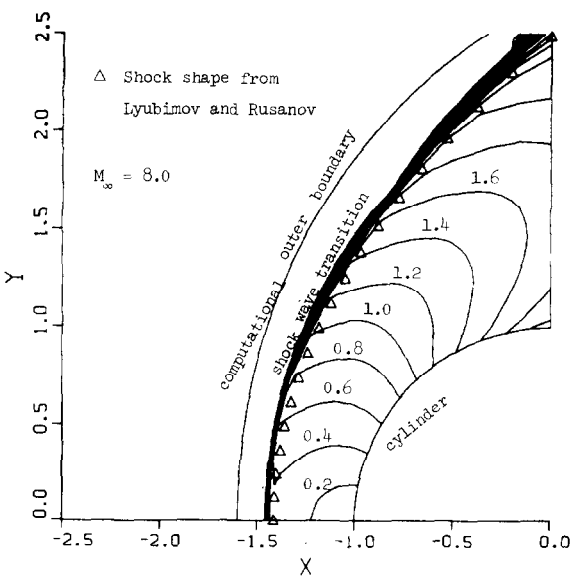

FIG. 9. Mach number contour plot for supersonic flow past circular cylinder ($M_\infty = 8.0$).

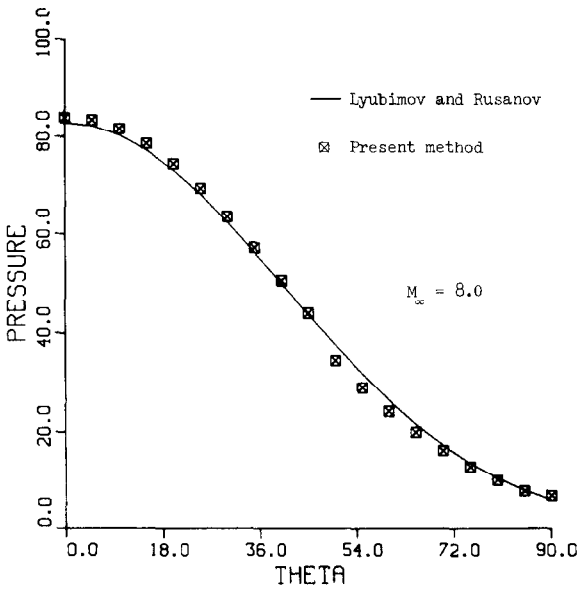

FIG. 10. Surface pressure distribution for supersonic flow past circular cylinder ($M_\infty = 8.0$).

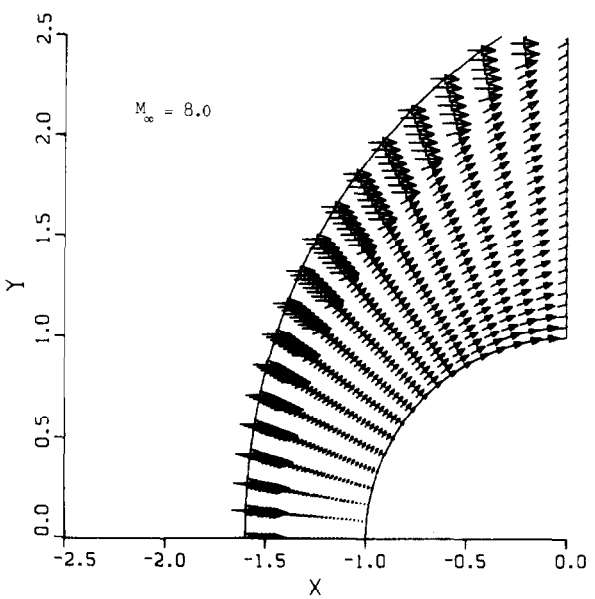

FIG. 11. Velocity vector plot for supersonic flow past circular cylinder ($M_\infty = 8.0$).

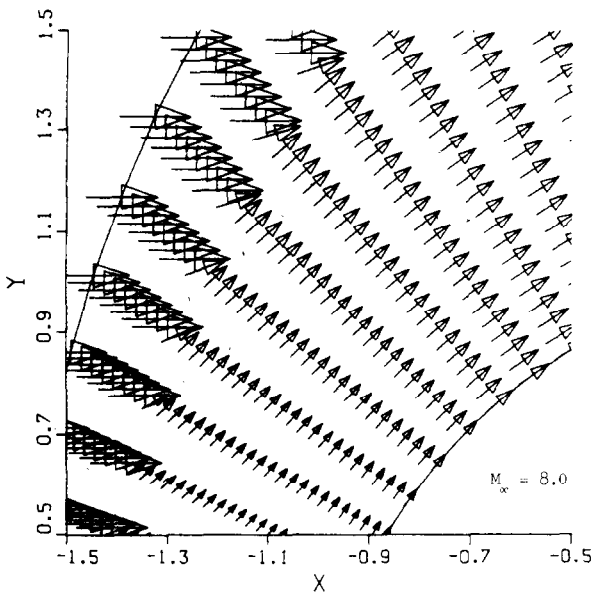

FIG. 12. Closeup of velocity vector plot.

observed. There is, however, a sudden change in the pressure gradient at $\theta = 45$–$50°$ on the sonic line. This is the expansion shock of magnitude $O(\Delta x)$, well-known for Godunov-type methods satisfying the entropy condition. If the entropy condition is violated, the jump may be $O(1)$; see [22]. As a final demonstration of our results for this problem, Figs. 11 and 12 show the velocity field about the circular cylinder. The arrows shown represent the direction of flow by their orientation and the magnitude by their length. They are drawn centered at grid points. The sharp deceleration and deflection of the flow by the oblique shock are clearly seen.

VII. Comparisons and Concluding Remarks

A comparison of the first author's scheme with Godunov's and Roe's can be summarized as follows.

(1) Osher's scheme is a first order, "monotone," upwind scheme in conservation form. Its use of simple waves rather than Hugoniot curves yields a simpler algorithm than Godunov's, and enables general geometries to be easily treated.

In the case of a single steady shock, Osher's scheme will, in general, have two transition zones with $(d-1)$ independent quantities varying over a single zone. Roe's and Godunov's will in general have one transition zone.

These upwind schemes admit a natural and general treatment of boundary conditions.

(2) The smoothness property mentioned above may make Osher's scheme better suited for use in an implicit mode.

(3) Unlike Roe's scheme, Osher's scheme satisfies the entropy condition for systems of equations in several space dimensions. Roe's scheme can be fixed to remove steady expansion shocks in one space dimension [22].

(4) For Euler's equations, Osher's scheme requires evaluation of the flux function at two intermediate state points per grid point, while Roe's requires one such evaluation, in addition to the necessary expansion shock corrector. This is assuming no sonic points are present. Both schemes require an additional flux evaluation in the presence of a sonic point.

For future work, it should be noted that both Osher's and Roe's schemes allow relatively simple field by field nonlinear decompositions. This allows the construction of second order accurate bounded variation extensions.

APPENDIX

Let (4.2) be approximated by (4.3) for the ξ derivative, with analogues for the η and ζ derivatives. Let the τ approximate derivative be taken in any conservative consistent way. Then we have:

THEOREM A.1. *Suppose* $q^n_{jkl} \to q(\xi, \eta, \zeta, \tau)$ *bounded almost everywhere as* $\Delta\xi, \Delta\eta, \Delta\zeta, \Delta\tau \to 0$. *Then* q *is a weak solution of* (4.2).

Proof. We suppress the k, l, n indices and show that, for any $\Phi(\xi) \in C_0^\infty$:

$$\sum_{j=-\infty}^{\infty} \Phi(\xi_j) \left[\int_{q_{j-1}}^{q_j} ((\xi_x)_j A(q) + (\xi_y)_j B(q) + (\xi_z)_j C(q) + (\xi_t)_j I)^+ \, dq \right.$$
$$\left. + \int_{q_j}^{q_{j+1}} ((\xi_x)_j A(q) + (\xi_y)_j B(q) + (\xi_z)_j C(q) + (\xi_t)_j I)^- \, dq \right] \tag{A.1}$$
$$\to \int_{-\infty}^{\infty} d\xi \left[E(q) \frac{\partial}{\partial \xi} (\xi_x \Phi) + F(q) \frac{\partial}{\partial \xi} (\xi_y \Phi) + G(q) \frac{\partial}{\partial \xi} (\xi_z \Phi) + qI \frac{\partial}{\partial \xi} (\xi_t \Phi) \right].$$

The remainder of the proof will follow in an obvious fashion.
We may rewrite the expression on the left in (A.1) as

$$\sum_{j=-\infty}^{\infty} \Phi(\xi_j) \left[(\xi_x)_j \left(\frac{E(q_{j+1}) - E(q_{j-1})}{2} \right) + (\xi_y)_j \left(\frac{F(q_{j+1}) - F(q_{j-1})}{2} \right) \right.$$
$$\left. + (\xi_z)_j \left(\frac{G(q_{j+1}) - G(q_{j-1})}{2} \right) + (\xi_t)_j \left(\frac{q_{j+1} I - q_{j-1} I}{2} \right) \right] \tag{A.2}$$

$$+\sum_{j=-\infty}^{\infty}\Phi(\xi_j)\left[-\int_{q_j}^{q_{j+1}}|(\xi_x)_j A(q)+(\xi_y)_j B(q)+(\xi_z)_j C(q)+(\xi_t)_j I|\,dq\right.$$

$$\left.+\int_{q_{j-1}}^{q_j}|(\xi_x)_j A(q)+(\xi_y)_j B(q)+(\xi_z)_j C(q)+(\xi_t)I|\,dq\right]$$

$$=I+II.$$

We must merely show that the second term, II, approaches zero as $\Delta\xi\to 0$. We may rearrange the sum to arrive at

$$II=\sum_{j=-\infty}^{\infty}\left[\int_{q_{j-1}}^{q_j}|(\xi_x)_j A(q)+(\xi_y)_j B(q)+(\xi_z)_j C(q)+(\xi_t)_j I|\,dq\right][\Phi(\xi_j)-\Phi(\xi_{j-1})]$$

$$-\sum_{j=-\infty}^{\infty}\Phi(\xi_j)\left(\int_{q_j}^{q_{j+1}}|(\xi_x)_j A(q)+(\xi_y)_j B(q)+(\xi_z)_j C(q)+(\xi_t)_j I|\right.$$

$$\left.-|(\xi_x)_{j+1}A(q)+(\xi_y)_{j+1}B(q)+(\xi_z)_{j+1}C(q)+(\xi_t)_{j+1}I|\,dq\right).$$

Since Φ is smooth with compact support, and the integrals are bounded by $K|q_j-q_{j-1}|$, for K a universal constant, the first term approaches zero, as a consequence of the Lebesgue dominated convergence theorem.

Also, since $||a|-|b||\leqslant|a-b|$, each of the second set of integrals is bounded by $K\,\Delta\xi\,|q_{j+1}-q_j|$. Thus, the second term goes to zero, for the same reason as above.

Next we have similar result for other approximations. Let (4.2) be approximated by (4.5) as above. We have:

THEOREM A.2. *Given the convergence hypothesis of Theorem* A.1, *then q is a weak solution of* (4.2).

Proof. This will follow the method of the proof above if we can show that

$$\sum_{j=-\infty}^{\infty}(\Phi(\xi_j)-\Phi(\xi_{j-1}))\left(\int_{q_{j-1}}^{q_j}((\xi_x)_{j-1/2}A(q)+(\xi_y)_{j-1/2}B(q)\right.$$

$$\left.+(\xi_z)_{j-1/2}C(q)+(\xi_t)_{j-1/2})^+\,dq\right)\to 0. \tag{A.4}$$

This follows in a familiar fashion from the Lebesgue dominated convergence theorem.

Finally, we can show an analogous result for (4.7) as an approximation to (4.6). We omit the (familiar and easy) details here.

ACKNOWLEDGMENT

We would like to thank Bram van Leer for his very helpful comments on a first draft of this paper.

REFERENCES

1. L. ABRAHAMSSON AND S. OSHER, to appear.
2. S. R. CHAKRAVARTHY, D. A. ANDERSON, AND M. D. SALAS, "The Split Coefficient Method for Hyperbolic Systems of Gas Dynamic Equations," AIAA Paper 80-0268, Pasadena, CA, 1980.
3. S. CHAKRAVARTHY AND S. OSHER, "Numerical Experiments with the Osher Upwind Scheme for the Euler Equations," AIAA Paper 82-0975, St. Louis, MO, 1982.
4. R. COURANT, E. ISAACSON, AND M. REES, *Comm. Pure Appl. Math.* **5** (1952), 243–255.
5. B. ENGQUIST AND S. OSHER, *Math. Comp.* **34** (1980), 45–75.
6. B. ENGQUIST AND S. OSHER, "One Sided Difference Schemes and Transonic Flow, Proceedings, National Academy of Sciences, Vol. 77, pp. 3071–3074, Washington, D.C., 1980.
7. B. ENGQUIST AND S. OSHER, *Math. Comp.* **36** (1981), 321–352.
8. S. K. GODUNOV, *Mat. Sb.* **47** (1959), 271–290.
9. P. M. GOORJIAN AND R. VAN BUSKIRK, "Implicit Calculations of Transonic Flow Using Monotone Methods, AIAA Paper 81–331, 1981.
10. A. JAMESON, *in* "Numerical Solutions of Partial Differential Equations III," pp. 275–320, Academic Press, New York, 1976.
11. P. D. LAX, "Hyperbolic Systems of Conservation Laws and the Mathematical Theory of Shock Waves," SIAM Regional Conf. Series Lectures in Appl. Math., Vol. 11, Philadelphia, PA, 1972.
12. P. D. LAX AND B. WENDROFF, *Comm. Pure Appl. Math.* **13** (1960), 217–237.
13. DAQUAN LI AND WENCI YU, *Sci. Sinica* **23** (1980), 1357–1367.
14. E. MURMAN, *AIAA J.* **12** (1974), 626–663.
15. J. OLIGER AND A. SUNDSTRÖM, *SIAM J. Appl. Math.* **351** (1978), 419–446.
16. S. OSHER, "Numerical Solution of Singular Perturbation Problems and Hyperbolic Systems of Conservation Laws," North-Holland Mathematical Studies 47, pp. 179–205, North-Holland, Amsterdam, 1981.
17. S. OSHER AND B. ENGQUIST, to appear.
18. A. N. LYUBIMOV AND V. V. RUSANOV, "Gas Flows Past Blunt Bodies," NASA-TT-F 715, February 1973.
19. S. OSHER AND F. SOLOMON, *Math. Comp.* **38** (1982), 335–374.
20. J. L. STEGER AND R. F. WARMING, "Fluw Vector Splitting of the Inviscid Gas Dynamic Equations with Applications to Finite Difference Methods," NASA Technical Memorandum 78605, 1979.
21. P. L. ROE, *J. Comp. Phys.*, in press.
22. B. VAN LEER, *SIAM J. Sci. Stat. Comp.*, in press.
23. S. K. GODUNOV, A. V. ZABRODIN, AND G. P. PROKOPOV, *USSR Comp. Math. Math. Phys.* **1**(1962), 1187–1219.
24. B. VAN LEER, *J. Comp. Phys.* **23** (1977), 263–275.
25. A. HARTEN, "On the Symmetric Form of Systems of Conservation Laws with Entropy," *ICASE Report #81-34* (1981).